Fibrinogen, Riboflavin, and UVA to Immobilize a Corneal Flap—Conditions for Tissue Adhesion

Stacy L. Littlechild,[1,2] *Gage Brummer,*[1,2] *Yuntao Zhang,*[1] *and Gary W. Conrad*[1,2]

Purpose. Laser-assisted in situ keratomileus (LASIK) creates a permanent flap that remains non-attached to the underlying laser-modified stroma. This lack of permanent adhesion is a liability. To immobilize a corneal flap, a protocol using fibrinogen (FIB), riboflavin (RF), and ultraviolet (UVA) light (FIB+RF+UVA) was devised to re-adhere the flap to the stroma.

Methods. A model flap was created using rabbit (*Oryctolagus cuniculus*) and shark (*Squalus acanthias*) corneas. Solutions containing FIB and RF were applied between corneal strips as glue. Experimental corneas were irradiated with long wavelength (365 nm) UVA. To quantify adhesive strength between corneal strips, the glue-tissue interface was subjected to a constant force while a digital force gauge recorded peak tension.

Results. In the presence of FIB, substantive non-covalent interactions occurred between rabbit corneal strips. Adhesiveness was augmented if RF and UVA also were applied, suggesting formation of covalent bonds. Additionally, exposing both sides of rabbit corneas to UVA generated more adhesion than exposure from one side, suggesting that RF in the FIB solution catalyzes formation of covalent bonds at only the interface between stromal molecules and FIB closest to the UVA. In contrast, in the presence of FIB, shark corneal strips interacted non-covalently more substantively than those of rabbits, and adhesion was not augmented by applying RF+UVA, from either or both sides. Residual RF could be rinsed away within 1 hour.

Conclusions. Glue solution containing FIB and RF, together with UVA treatment, may aid immobilization of a corneal flap, potentially reducing risk of flap dislodgement. (*Invest Ophthalmol Vis Sci.* 2012;53:4011–4020) DOI:10.1167/iovs.12-9515

From the [1]Division of Biology, Kansas State University, Manhattan, Kansas; and [2]Mount Desert Island Biological Laboratory, Salisbury Cove, Maine.

Supported by an Undergraduate Outreach Fellowship from the NIH/NCRR Maine IDeA Network of Biomedical Research Excellence (ME-INBRE: 2-P20-RR016463); Johnson Center for Basic Cancer Research, Kansas State University; NIH-NEI grant NIH EY0000952 (GWC); and K-INBRE Award Number P20-RR016475 from the National Center for Research Resources. The content is solely the responsibility of the authors and does not necessarily represent the official views of the National Center for Research Resources or the National Institutes of Health.

Submitted for publication January 16, 2012; revised March 23 and May 1, 2012; accepted May 4, 2012.

Disclosure: **S.L. Littlechild**, None; **G. Brummer**, None; **Y. Zhang**, None; **G.W. Conrad**, None

Corresponding author: Stacy L. Littlechild, Division of Biology – Ackert Hall, Kansas State University, Manhattan, KS 66506-4901; Telephone 785-769-3376; stacy.little08@gmail.com.

Clinical laser-assisted in situ keratomileus (LASIK) protocols use a microkeratome blade or femtosecond laser to create a 100–180 μm deep lateral incision into the corneal stroma to separate a top layer of the stroma, while leaving it connected, via a non-incised region, to an underlying bottom layer of stroma, much like a door is left connected to the frame by a hinge.[1–4] Once this flap is created, the underlying stroma is exposed and reshaped using a laser to vaporize a calculated amount of the bottom stromal layer. After the cornea is reshaped, the stromal flap is re-applied smoothly on top of the bottom layer of underlying stroma to correct eye conditions, such as nearsightedness, farsightedness, or astigmatism. LASIK patients have experienced complications, such as dislocation of the flap up to 9 years postoperatively upon head/corneal trauma[5–8] and recurrent epithelial ingrowth,[9–10] yet to our knowledge there is no standard treatment to ensure that the flap re-adheres to or is immobilized to the lower surface, other than by surface tension. Furthermore, a study of the local keratan sulfate and chondroitin/dermatan sulfate disaccharides in human postmortem, post-LASIK corneas suggests that the reason why the LASIK flap never heals to the underlying stroma is that exposure to the laser irradiation alters permanently the composition of the glycosaminoglycans on the modified surface of the stroma[11] and renders it non-functional for normal wound healing adhesion.

Our study uses a combination of fibrinogen (FIB), riboflavin (RF), and long wavelength (365 nm) ultraviolet light (UVA) to create a "biologic tissue glue" to adhere the stromal layers of a corneal flap to the exposed bottom stromal layer, and thus decrease the risk of flap dislodgement and re-exposure of the underlying stroma.[12] Experiments performed on rabbit and shark corneas were designed to create a beginning model of a cornea containing a LASIK flap. The model reported describes the covalent and non-covalent interactions between an anterior corneal stromal flap and the underlying stromal bed still containing native macromolecules, not yet modified by the effects of laser ablation used in the LASIK protocol demonstrated previously to alter their composition significantly.[11] Therefore, in the interests of accuracy, the corneas prepared here are referred to as containing a "corneal flap," rather than a "LASIK flap."

Materials and Methods

Materials

FIB and "riboflavin" were purchased from Sigma (Cat. Nos. F8630 and 77623, respectively, the latter as riboflavin-5′-phosphate, the soluble compound that generates genuine riboflavin in solution; St. Louis, MO). Solutions of riboflavin-5′-phosphate will be referred to here as "riboflavin" (RF). Dextran was purchased from Fisher Scientific (Cat. No. BP1580; Pittsburgh, PA). Rabbit eye globes were purchased from Pel Freez Biologicals (Catalog No. 41211-2; Rogers, AR).

Solution Preparation

Experimental solutions used for adhesion testing were prepared fresh before experimentation, and included "FIB only," "RF only," and "FIB+RF." FIB solutions contained 18% (wt/vol, 180 mg/mL, 530 μM) FIB. RF solutions contained 2.6% (wt/vol, 2.6 mg/mL, 5.44 mM) of RF. De-ionized water was used as the solvent in all experimental solutions, as per the protocol of Khadem et al.[12] All experimental solution tubes were wrapped in aluminum foil following preparation to prevent premature photoactivation of RF. A 20% (wt/vol, 400 nM) dextran in 1× PBS (pH 7.2) solution was applied topically to keep rabbit and shark corneas from drying during experimentation.

Tissue Preparation

Corneas from spiny dogfish sharks, *Squalus acanthias*, were harvested at Mount Desert Island Biological Laboratory, Salisbury Cove, ME, and Marine Biological Laboratory, Woods Hole, MA, under an Institutional Animal Care and Use Committee (IACUC) and ARVO Animal Statement for the Use of Animals in Ophthalmic and Vision Research approved protocol. Within 5 minutes of euthanization, corneas were dissected from sharks and snap-frozen using liquid nitrogen. Corneas then were stored in a −80°C freezer until needed for experimentation. Rabbit eye globes were ordered from Pel-Freez Biologicals, stored in −80°C until needed for experimentation, and then thawed partially to allow dissection of the corneas surrounded by a 6 mm wide margin of sclera.

At Kansas State University, shark corneas were placed in 1 × PBS (pH 7.2) to thaw. Next, shark corneas were de-epithelialized and de-endothelialized using a spatula (Fig. 1a).[13] Then, two 8 mm-wide strips were excised from the centermost region of the cornea using a razor blade (Fig. 1b). To ensure the strips consistently were 8 mm wide, a visible guide was placed beneath the cornea and Petri dish to indicate where each cornea should be cut to produce strips of identical widths. Once two strips were isolated from the central region of the shark cornea, one of the strips was rotated laterally so as to match the orientation of the other strip (Fig. 1c). Next, one "scleral tag" was removed from opposite ends of each strip (Fig. 1d) to prevent adhesion from occurring between surfaces that were not cornea-to-cornea (e.g., sclera-to-sclera).

Rabbit corneas were treated identically to shark corneas except, because of the smaller size of the rabbit eye globe, only one 8 mm strip was excised from the center region of each cornea (Fig. 1b′). Therefore, in rabbits, 2 whole eye globes were used to create 1 experimental pair, whereas only 1 eye globe was sufficient to create the experimental pair in sharks.

Additional testing was performed on rabbit corneas to determine the effect of the presence/absence of Descemet's membrane (DM) and of corneal orientation on strip adhesion. In orientation 1 (DM:epithelial basement membrane [Epi-BM]), rabbit corneas were placed on top of each other in the same orientation (anterior surfaces facing up), so the posterior surface of the top strip (DM) interacted with the anterior surface of the bottom strip (Epi-BM, Fig. 2a). In orientation 2 (stroma:Epi-BM), rabbit corneas were placed on top of each other (anterior surfaces [Epi-BM] facing up), except the DM was removed gently with jeweler's forceps from the posterior surface of the top strip. In this orientation, the posterior surface of the top strip (exposed stroma) interacted with the anterior surface of the bottom strip (Epi-BM, Fig. 2b). In orientation 3 (stroma:stroma), the anterior surface Epi-BMs were left intact, but the DM was removed from the posterior surfaces of both strips. After flipping over the bottom strip, the two posterior surfaces (both exposed stromas) of the top and bottom corneal strips interacted in this orientation (Fig. 2c), thus approximately modeling the stroma-to-stroma interaction of a LASIK cornea (but absent the laser-modification of the bottom layer surface).

Tissue Treatment

Following corneal strip excision, 30 μL of experimental solution were distributed evenly on what became the "lower strip" of each set (Fig. 3a), and the remaining strip was placed on top to represent a corneal flap (Fig. 3b). During experimentation, the aforementioned system, consisting of two strips of cornea with solution in between, was placed on a contoured surface to resemble the natural curvature of the eye (Fig. 3c). This two-strip tissue "sandwich" or tissue pair was allowed to incubate for a total of 30 minutes to allow the solution/glue to penetrate somewhat into each tissue interface. To keep the tissue from drying during incubation, a 20% (wt/vol) dextran solution was dripped onto the surface using a syringe pump at a rate of 10 μL per minute (Model NE-4000; New Era Pump Systems, Inc., Farmingdale, NY, Fig. 3d). Upon completion of the permeation stage, experimental corneas were placed 50 mm beneath a light emitting diode and irradiated with long wavelength UVA (365 nm UVA, 3 mW/cm^2 intensity) for an additional 30 minutes (the dextran drip was continued at 10 μL per minute during irradiation, Fig. 3e). Control corneas also continued to receive the 20% dextran drip for the second 30-minute period, but were not exposed to UVA irradiation.

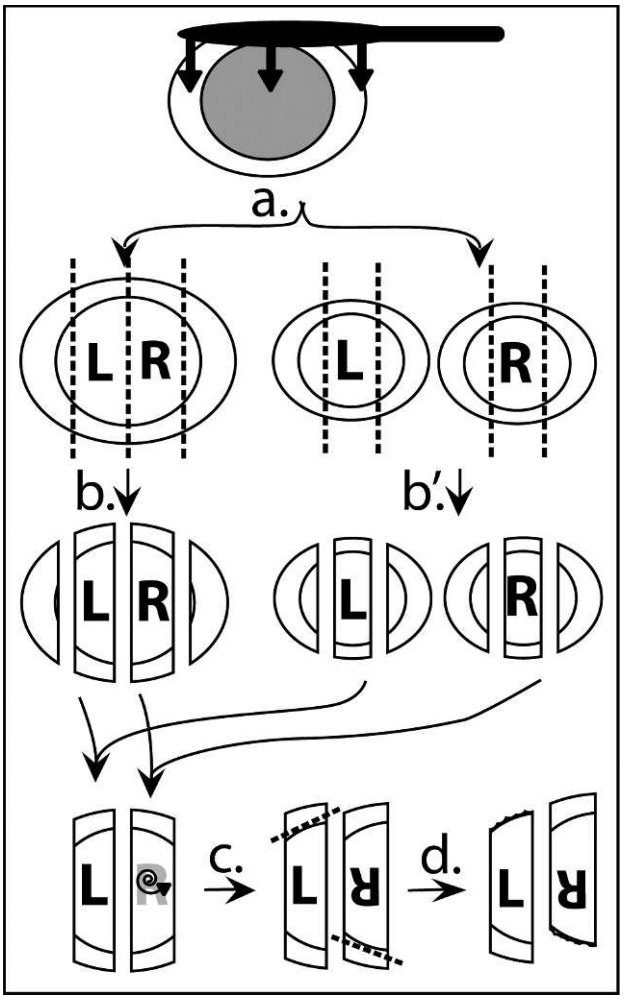

Figure 1. Tissue preparation. (**a**) Cornea was de-epithelialized using spatula. (**b**) De-epithelialized shark (**b′**) and rabbit corneas were cut into 8 mm strips from the centermost region using a razor blade. Two strips were harvested from each shark cornea; due to smaller size of rabbit eyes, only one 8 mm strip was isolated per cornea. (**c**) One cornea strip was rotated to match orientation of remaining strip. Both corneas remained epithelial-side up. (**d**) Scleral tags were removed on opposite ends of each strip to prevent adhesion between scleral tissue during testing.

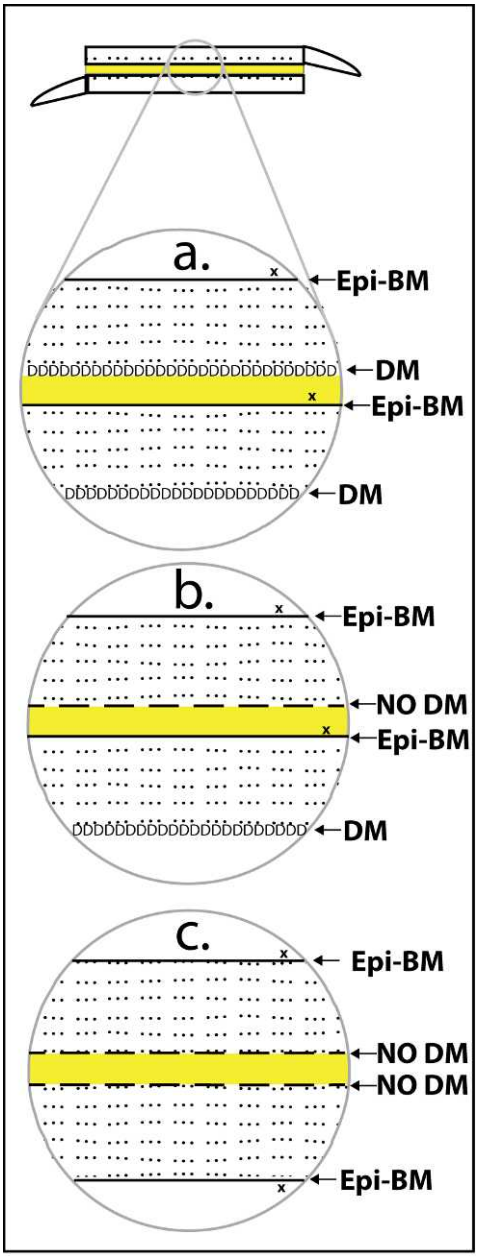

Figure 2. Tissue orientation. In all 3 orientations, the glue solution is represented by the yellow shaded zone. (**a**) Orientation 1 (DM:Epi-BM): Two rabbit cornea strips were stacked with anterior surfaces facing up. Epithelium was removed (*x*) from both strips. DM (*DDD*) was left intact in both strips. (**b**) Orientation 2 (stroma:Epi-BM): Two rabbit cornea strips were stacked with anterior surfaces facing up. Epithelium was removed from both strips. DM was removed from top strip to expose stromal ECM. (**c**) Orientation 3 (stroma:stroma): Two rabbit cornea strips were stacked with posterior surfaces facing each other. Epithelium was removed from both strips. DM was removed from both strips to expose stromal ECM.

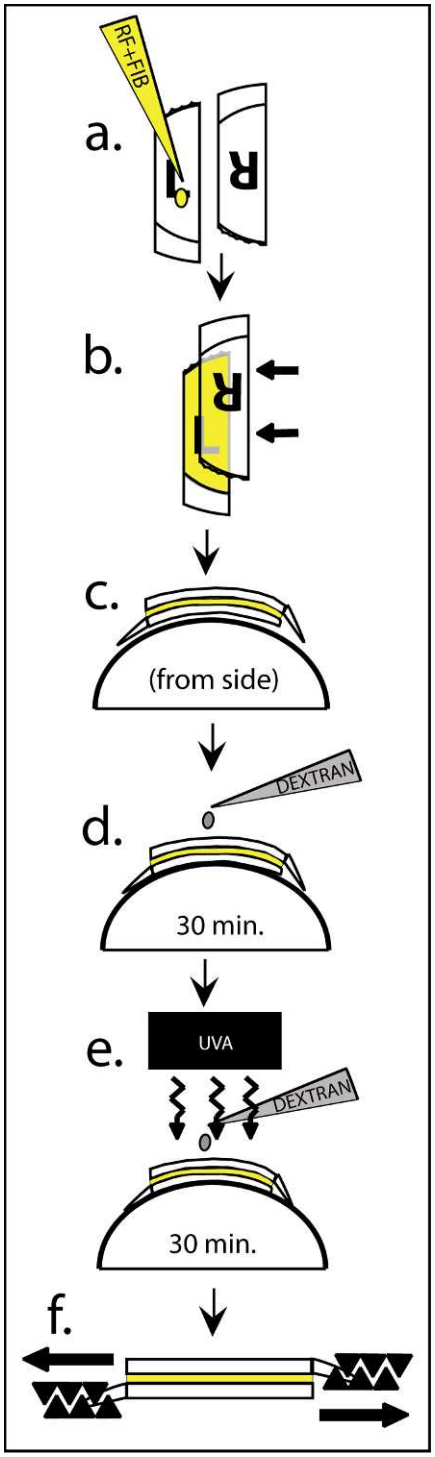

Figure 3. Tissue treatment/adhesion testing. (**a**) Control or experimental glue solution (here, the experimental solution is colored *yellow*, 30 μL) was dispensed using a pipette onto surface of what became the "bottom strip" of the system. (**b**) "Top" cornea strip then was placed on bottom strip, maintaining correct orientation. (**c**) Tissue pair was placed on top of a curved surface to model natural contour of the eye (*side view*). (**d**) Dextran solution (20% wt/vol) was applied topically to top of tissue pair for 30 minutes. (**e**) Experimental corneas then received 30 minutes of UVA irradiation. (**f**) Scleral tags were gripped and constant tension was applied horizontally in opposite directions for quantitative measurement of tissue-to-tissue adhesion strength.

Adhesion Testing

To measure quantitatively the force of adhesion generated by the glue, the scleral tag of one strip was clamped on one side and the tag of the other strip was clamped on the other side, thus creating a "nested" pair of corneal tissue strips. Constant tension then was applied horizontally to the two clamps at a rate of 6 mm/min (Motorized Horizontal Test Stand, Item ML275; Imada, Northbrook, IL, Fig. 3f). The

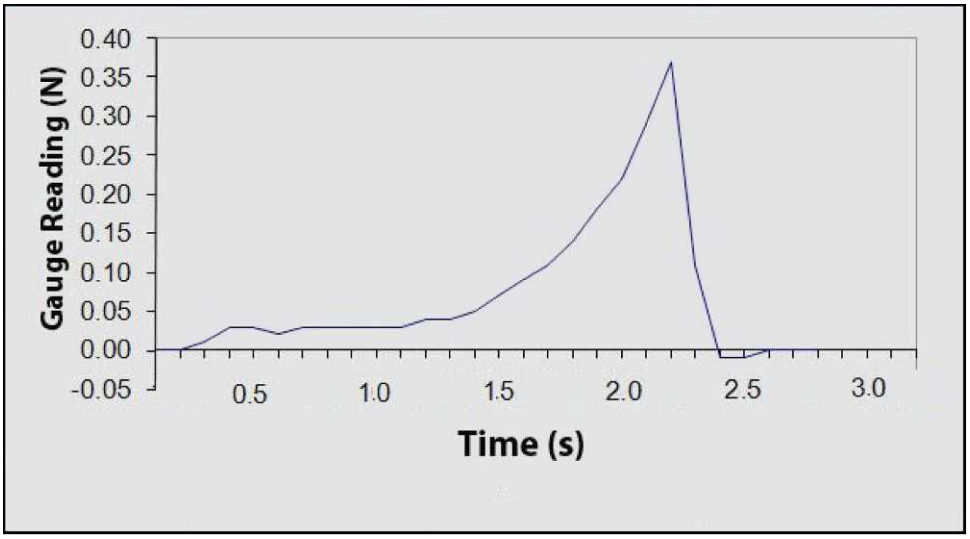

Figure 4. Sample graph. Imada software generated force versus time graph of increasing tension on treated pair of corneal strips until integrity of adhesion is overcome and strips slide apart by shearing along the glue interface. Gauge reading (*y-axis*) is adhesion force measured in Newtons. Time (*x-axis*) refers to real time measured in seconds.

pulling force, therefore, was applied directly to the adhesive interface between the two strips in a manner designed to determine the force needed to make the two surfaces break the adhesion and slide past each other. Computer software then interpreted the values collected every 0.10 second to generate a force versus time graph (Force Acquisition Software, Item SW-1; Imada, Fig. 4). Each measurement condition described in Figures 7 and 8 was repeated at least 8 times before calculating averages, standard deviations, and degrees of significant difference.

Post-Treatment Corneal Transparency

Because solutions containing RF have a yellow hue, it was important to observe corneal clarity following treatment to determine if transparency was compromised. Rabbit corneas were prepared in the stroma:stroma orientation as described above and imaged immediately following four separate treatments (none, FIB only, RF+UVA, and FIB+RF+UVA, Fig. 5a). Additionally, after corneal pairs were imaged immediately following treatment, the tissue was placed in 1 × PBS, subjected to gentle movement, and imaged again after 30 minutes and 1 hour of 1 × PBS incubation. The rinsing procedure showed how readily residual RF was rinsed from the treated tissue.

Image-analysis software (Image Pro; Media Cybernetics, Inc., Bethesda, MD) was used to quantify transparency of corneas prepared as described above. The protocol used has been described in detail previously.[14] In short, two images were collected: image 1 was of the cornea in a Petri dish of 1 × PBS (focused on the cornea), and image 2 was of the dish containing 1 × PBS without the cornea (this was the background image and was taken at the same focal level as when the cornea was present in the dish). Optical density of the corneas then was quantified by performing a background correction on the image of the cornea, converting the corrected image from an RGB-color image to a 16-pixel gray scale image, and finally measuring the light intensity of pixels in the selected area (the center) of the image. These data are shown in Figure 5b.

Tissue Imaging

To show the presence and absence of epithelium (EPI) and the DM following tissue isolation in a rabbit cornea, approximately 10 μm thick cryostat tissue sections were imaged (Model OTF; Bright Instrument Company LTD., Huntingdon, Cambridge, UK). Figure 6a shows the intact rabbit cornea with EPI and DM present. Figure 6b depicts a rabbit cornea following removal of epithelium with a spatula, and Figure 6c illustrates a rabbit cornea after removal of DM with jeweler's forceps.

Results

Adhesion Testing – Rabbit Corneas

Results collected from orientation 1 (DM:Epi-BM, Fig. 7a) suggest that, as predicted initially, greatest adhesion is achieved when FIB+RF+UVA are present during tissue treatment, with adhesion greater than any of the 7 types of control preparations of adhesive solutions. This indicates that, in this orientation where the two surfaces that interact with FIB+RF+UVA are both basement membranes, but unlike each other (DM:Epi-BM), protocol 8 (FIB+RF+UVA) produces the strongest adhesion, statistically significantly different from all other controls in this orientation, including the next strongest control, protocol 5 (FIB+RF). Orientation 1 (DM:Epi-BM) was used as a simple beginning point to study FIB-glue-mediated adhesion between two dissimilar basement membrane surfaces, even though the tissues apposed are not in the orientation of a LASIK cornea.

In proceeding stepwise to study adhesion with a new set of extracellular matrix (ECM) components, one surface from orientation 1 (Epi-BM) and the other, raw stroma, were tested in orientation 2 (stroma:Epi-BM, Fig. 7b). Surprisingly, data showed two new features. First, magnitudes of adhesion were dramatically higher in orientation 2, almost double the values observed in orientation 1. In comparison with orientation 1, FIB+RF+UVA conditions led to higher absolute levels of adhesion (orientation 1: 0.08 Newtons [N] versus orientation 2: 0.12 N). Secondly, surprisingly, two other protocols showed adhesion as strong as protocol 8 (protocols 2 [FIB] and 6 [FIB+UVA]). Both involve FIB, as does protocol 8. Because FIB alone (protocol 2) generated adhesion levels as high as FIB+UVA (protocol 6) and those levels were as high as FIB+RF+UVA (protocol 8), the simplest conclusion is that orientation 2 (stroma:Epi-BM) has revealed a new type of adhesion that does not involve the formation of covalent cross-links and involves the stroma. This conclusion can be drawn because, in the case of FIB alone (protocol 2), there is no RF or

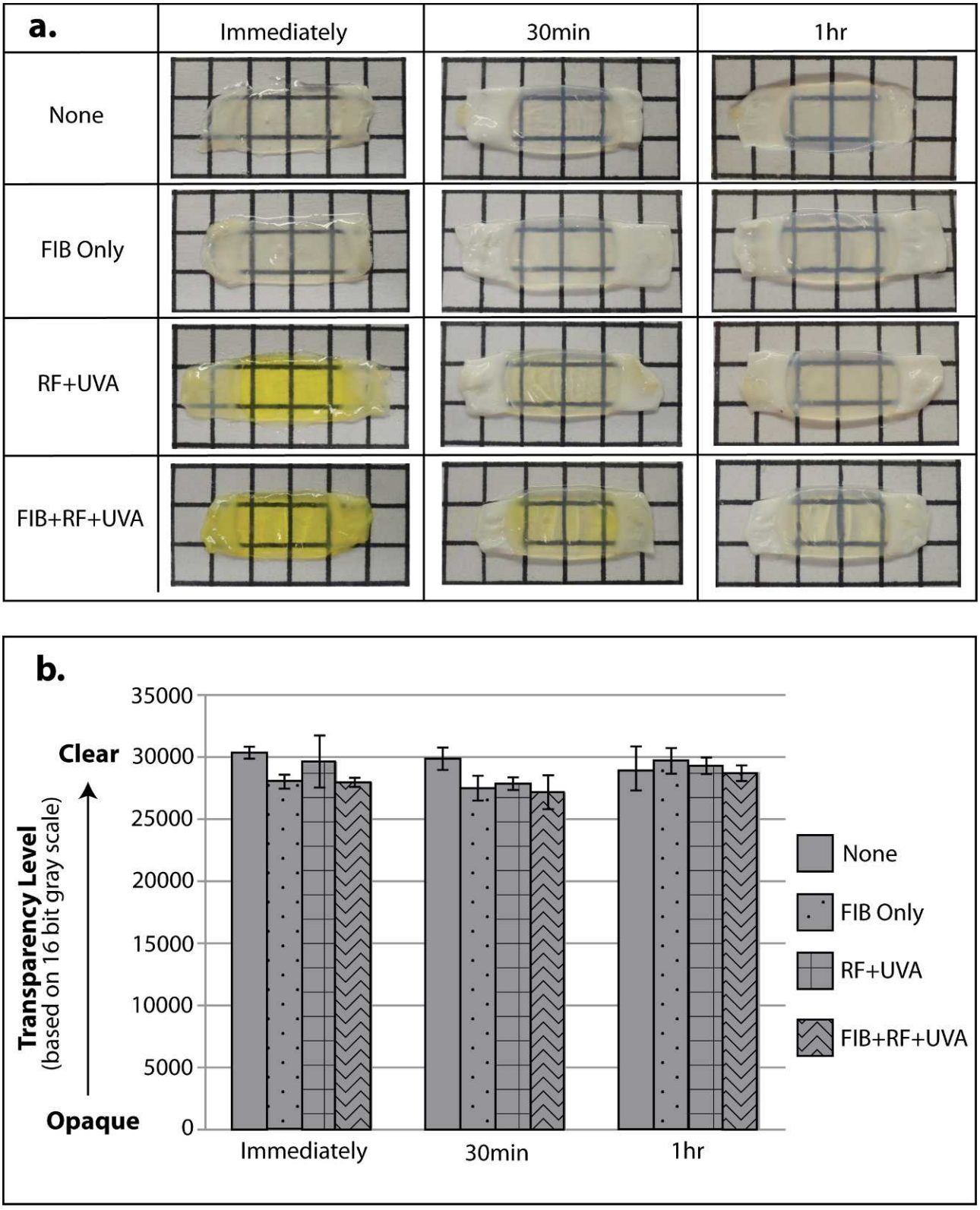

Figure 5. Corneal transparency. (**a**) Corneal strips were placed on a grid immediately following treatment and after incubation in 1 × PBS for 30 minutes and 1 hour to visualize the effect of respective treatments on corneal transparency. (**b**) Optical density of corneas was measured with imaging software to quantify transparency changes immediately after treatment, and 30 minutes and 1 hour after 1 × PBS rinse.

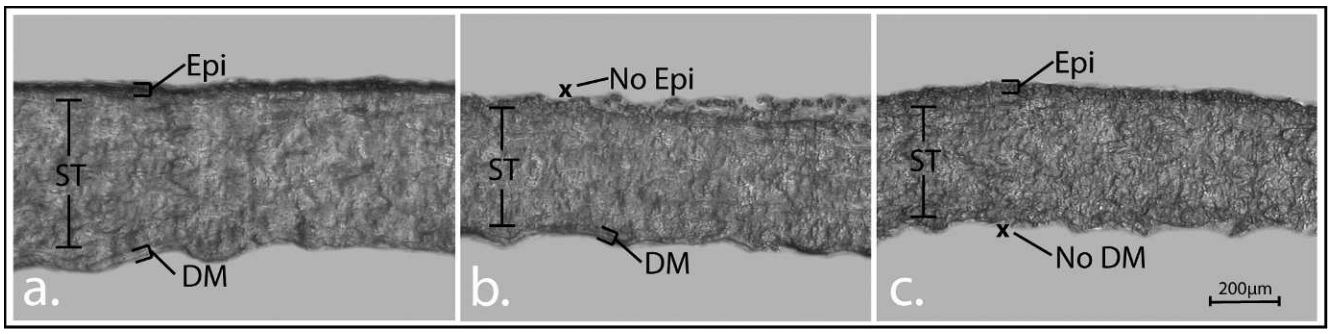

Figure 6. Rabbit cornea cross sections. Epithelium (*Epi*) is present in (**a**) and (**c**), but absent in (**b**). DM is present in (**a**) and (**b**), but absent in (**c**). Stroma (*ST*) remains intact in (**a–c**). Bar length in bottom right corner of (**c**) represents 200 μ.

UVA to catalyze formation of covalent cross-links, yet its adhesion is of the same magnitude as protocols 6 (FIB+UVA) and 8 (FIB+RF+UVA). All that is different in orientation 2 is that the absence of the DM allows ECM molecules in the stroma to participate in the adhesion, albeit from only one side of the glue layer.

The remarkably increased adhesion observed in orientation 2 (stroma:Epi-BM) upon removal of DM and the consequent exposure of raw stroma in one strip, thus, suggested that the exposure of two stromal surfaces to each other via removal of both DMs in orientation 3 (stroma:stroma) might generate even greater adhesion. The result, as predicted, was even higher tissue adhesion achieved as a result of orienting corneal strips so two stromal surfaces interacted with FIB glue (Fig. 7c). To determine the extent to which adhesion of protocol 8 (FIB+RF+UVA) was RF-UVA-catalyzed, covalent adhesion, it was important to look at the amount of adhesion seen in the absence of RF and UVA. Protocol 2 (FIB) in Figure 7c revealed that even FIB alone, in the absence of RF and UVA, produced extremely high adhesion (0.29 N in orientation 3 vs. 0.15 N in orientation 2 vs. 0.03 N in orientation 1). This indicates that in a stroma:stroma interaction, FIB alone generates very strong non-covalent adhesion. However, Figure 7c also shows evidence for an additional type of adhesion that *is* UVA-catalyzed and covalent: when FIB interacted with two stromal surfaces and also then was irradiated with UVA light (both in the presence or absence of RF, protocols 6, 8), the level of adhesion was markedly higher. This UVA-induced adhesion is presumed to be covalent (mechanism in Discussion) and reaches almost twice the degree of adhesion as FIB alone. As shown in Figure 7c, all of those adhesions involving stroma:stroma interactions in the presence of FIB are orders of magnitude greater than those seen in orientation 1 or 2. That comparison of the adhesive strengths measured between strips of rabbit corneas in orientations 1–3 is seen most dramatically when the data from all 3 orientations are graphed on the same scale (Fig. 7d).

Test of UVA Penetration – Rabbit Corneas

In exploring ways that adhesion seen in protocol 8 (FIB+RF+UVA) could be increased even further, it was reasoned that, especially in the presence of RF, covalent cross-links probably formed near the stroma interface with the FIB glue closest to the UVA source. This is logical because RF not only acts as a catalyst for cross-link formation, but also blocks UV penetration into deeper layers,[15] leading us to hypothesize that in the presence of RF, UVA does not penetrate the glue layer substantively to the other glue:stroma interface. Therefore, to test this hypothesis without increasing the total UV dosage, we exposed one side of the corneal set for 15 minutes, then gently flipped the pair of corneal strips over (without allowing their separation) and exposed the opposite side for an additional 15 minutes (Fig. 7c, protocol 9). Results obtained from orientation 3 (stroma:stroma), protocol 9 (FIB+RF+UVA 15 mins/side) were consistent with this hypothesis, because the degree of adhesion increased spectacularly to the highest level ever observed in rabbit corneas (1.00 N).

Adhesion Testing – Shark Corneas

As in orientation 3 (stroma:stroma) of rabbit cornea trials, when shark corneal stromas were allowed to interact directly, they demonstrated that FIB alone (protocol 2) and FIB+RF (protocol 5) produced adhesion as strong as that of protocol 8 (FIB+RF+UVA, Fig. 8). As in rabbit corneas, protocol 8 (FIB+RF+UVA) gave adhesion substantially greater than protocol 1 (none), 3 (RF alone), or even 7 (RF+UVA). Also similar to rabbits, the simple addition of FIB to the treatment led to very strong stromal adhesion. However, in the case of shark corneas, the data suggested that all adhesion seen in orientation 3 (stroma:stroma) is non-covalent because in the presence of RF and UVA, there is no significant increase in adhesion. This led to a prediction that if no covalent adhesion is occurring in shark corneas in response to RF+UVA, adhesion would *not* increase as it does in rabbit tissue if both sides of the shark corneal tissue pair were irradiated with UV.

Test of UVA Penetration – Shark Corneas

Results from protocol 9 (FIB+RF+UVA 15 mins/side) of orientation 3 (stroma:stroma) in shark tissue supported this hypothesis: there was no substantial increase in adhesion when both sides of system were exposed to UV (Fig. 8), indicating that only very strong, non-covalent adhesion takes place between the FIB glue and the shark corneal stroma, rather than the covalent *and* non-covalent adhesion mechanisms that are responsible for adhesion between the FIB glue and the rabbit corneal stroma. Note that the ranges of all those protocols involving application of FIB to shark corneas (protocols 2, 5, 6, 8, 9) generated levels of adhesion (1.0–3.0 N) that were triple those seen using rabbit corneas, even including the additional effects from RF+UVA.

Post-Treatment Corneal Transparency

Images collected from treated corneal pairs showed that if RF was present during treatment, the corneas had a fluorescent yellow color (Fig. 5a). However, after 30 minutes of incubation in 1 × PBS, most of the RF was rinsed away and only a subtle yellow hue remained. Moreover, after an additional 30 minutes (total of 1 hour) incubation in 1 × PBS, the transparency of the

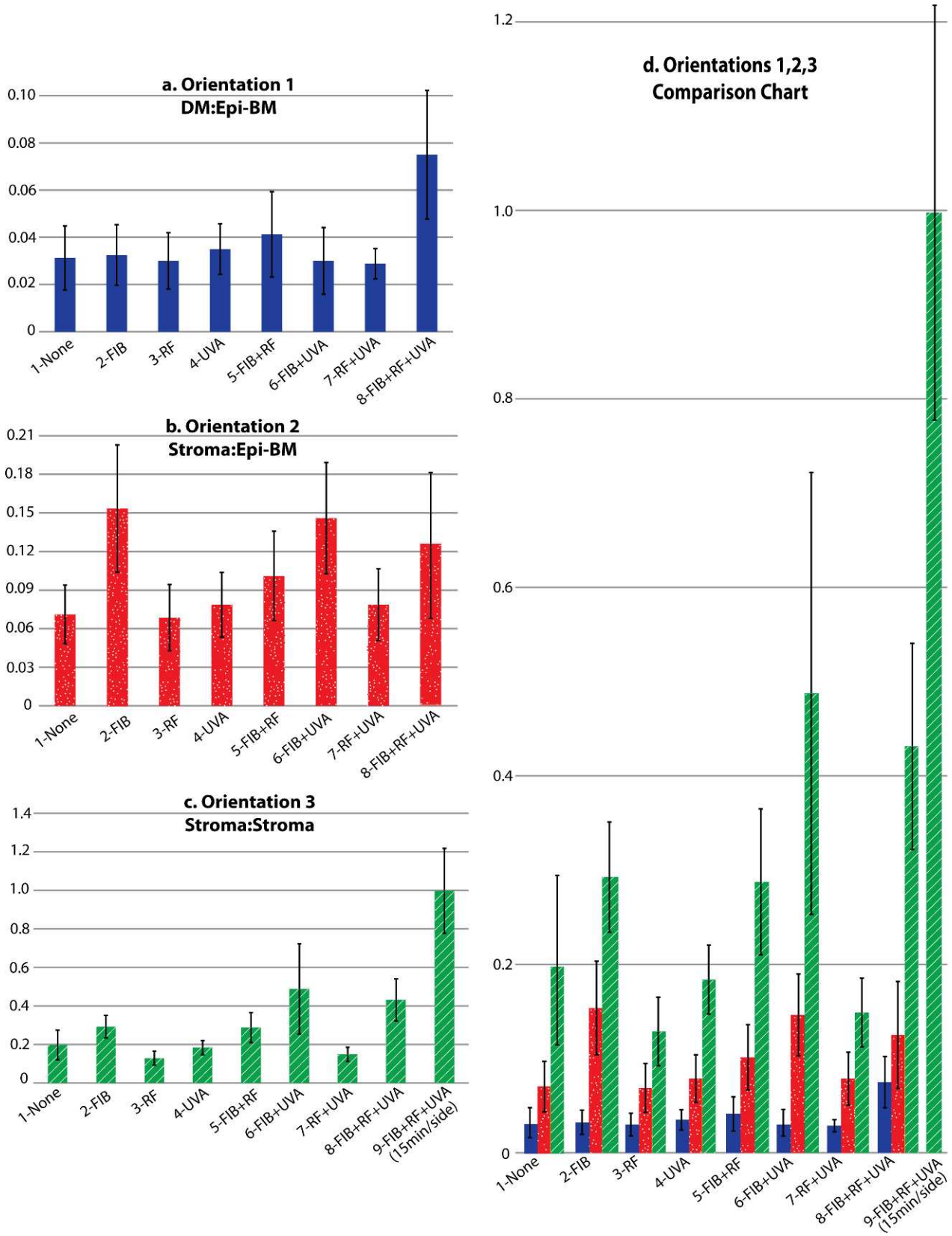

Figure 7. Rabbit cornea adhesion. All y-axis values are measured in Newtons (N). (**a**) Orientation 1 (DM:Epi-BM): Effects of FIB, RF, and UVA on rabbit corneas oriented so DM of top strip interacts with Epi-BM of bottom strip. Greatest adhesion is produced when FIB, RF, and UVA all are present. (**b**) Orientation 2 (stroma:Epi-BM): Effects of FIB, RF, and UVA on rabbit corneas after removal of DM from top strip. One stromal surface interacted with epithelial BM of bottom strip. Most adhesion occurred in protocols that contained FIB (2, 5, 6, 8). (**c**) Orientation 3 (stroma:stroma): Effects of FIB, RF, and UVA on rabbit corneas after DM was removed and bottom strip was flipped over so the two stromal surfaces interacted. Strongest adhesion occurred between FIB-containing protocols, as in orientation 2 (stroma:Epi-BM). New protocol 9 (FIB+RF+UVA, 15 mins/side)

was applied to the orientation 3 (stroma:stroma) "sandwich" to test the hypothesis described in Results section. (**d**) All data collected from rabbit corneas were compared along the vertical scale of one graph to demonstrate the dramatic increase in adhesion observed when one or both stromal surfaces were exposed and allowed to interact. *Averages and standard deviations are based on measurement of at least 8 replicates of each condition.

corneal pairs was restored almost totally to that of the "none" control, suggesting that residual RF could be rinsed easily from the treated corneas.

Additionally, *t*-test statistical analysis was performed on the quantitative transparency data in Figure 5b. The statistical analysis identified that the corneas treated with FIB only and FIB+RF+UVA were significantly more optically dense as compared to "none" corneas immediately following treatment. Interestingly, the optical density of the RF+UVA corneas immediately after treatment was not significantly different from the "none" control immediately after treatment, suggesting that, despite its yellow hue, the presence of RF in the treated cornea does not hinder overall clarity of the cornea. Furthermore, after 1 hour of 1 × PBS rinsing, the optical density of FIB only and FIB+RF+UVA corneas decreased, and their transparency no longer was statistically different from that of the "none" corneas.

Discussion

Development of a tissue glue to reinforce the LASIK flap would be invaluable to those patients who have received or plan to receive LASIK. Based on the data collected here, the application of such glue as a standard addition to current LASIK protocols would increase the amount of force required to dislodge a corneal flap, and/or would decrease the incidence of flap dislocation upon trauma to the eyes of postoperative patients. Additionally, epithelial ingrowth that results occasionally from LASIK likely would be reduced.

In developing a protocol to test the candidate tissue glue presented in our study, two model corneas (shark and rabbit) were studied. Shark and rabbit corneas have been used in previous corneal cross-linking studies and have produced results similar to each other.[16,17] Additionally, shark and rabbit corneas are large and easily accessible (when compared to those of other model organisms, such as the adult chicken or mice).

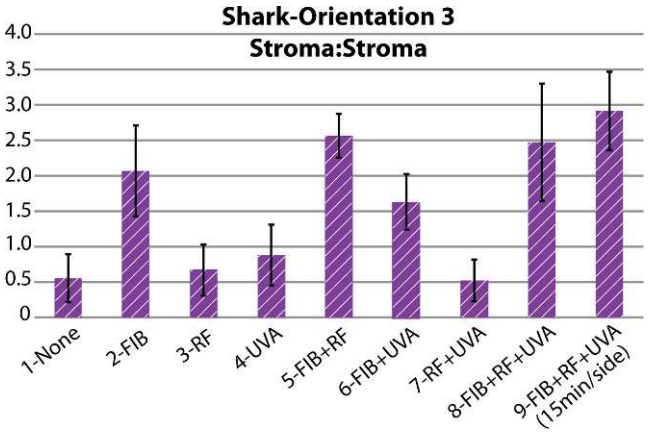

Figure 8. Shark cornea adhesion. All y-axis values are measured in Newtons (N). Effects of FIB, RF, and UVA on shark cornea stromal adhesion. DM was removed from both strips and oriented so both exposed stromal surfaces interacted with control or experimental solutions (Fig. 3c). Non-covalent adhesion occurred in controls containing FIB. The lack of strengthened adhesion in protocol 8 or 9 demonstrated that no covalent interactions were responsible for the adhesion that occurred in shark corneas. *Averages and standard deviations are based on measurement of at least 8 replicates of each condition.

It can be concluded from data collected from rabbit corneal strips in orientation 1 (DM:Epi-BM) that protocol 8 (FIB+RF+UVA) was the most effective at adhering the strips of the corneal pairs, suggesting its mechanism involves formation of covalent bonds. However, because after scraping away the endothelium, the DM was present on the posterior surface of the top strip, and because after scraping away the epithelium, the epithelial BM was present on the anterior surface of the bottom strip,[18,19] the FIB+RF+UVA would have been interacting on both surfaces with predominately BM proteins, such as collagen type IV and laminin, which are native to basement membranes.[20,21] These proteins are unlike those that would be available for interactions in the stroma of a LASIK patient because the LASIK flap is created intrastromally[22,23] and, in addition, has undergone significant molecular modification as a result of exposure to the laser.[11] Nonetheless, as a control, BM-BM adhesion levels were important to characterize.

Data collected from rabbit corneas in orientation 2 (stroma:Epi-BM) tested interactions between stromal ECM molecules, such as collagen type I[24]; proteoglycan core proteins (decorin, keratocan, and lumican), and glycosaminoglycans (keratan sulfate, chondroitin sulfate, dermatan sulfate, and heparan sulfate),[25] and, like those in orientation 1, epithelial basement membrane molecules collagen type IV and laminin. This change in the available molecular binding partners revealed an additional mechanism of adhesion that added to overall adhesive strength between the exposed stromal surface and the epithelial basement membrane. As in orientation 1 (DM:Epi-BM), protocol 8 (FIB+RF+UVA), generated very strong adhesion when compared to most other controls. Surprisingly, in addition, two other protocols, 2 (FIB) and 6 (FIB+UVA) demonstrated adhesion similar in strength to that of the FIB+RF+UVA protocol. Because no RF or UVA was involved to catalyze formation of covalent interactions in protocol 2 (FIB), the mechanism by which that adhesion occurred must have been non-covalent. A second prediction generated by the greatly enhanced adhesions seen in orientation 2 (stroma:Epi-BM) data, therefore, was that if more stromal ECM molecules were exposed, more adhesion would occur between FIB and corneal tissue, and thus generate even greater adhesion between the corneal strips. To test this hypothesis, which also most accurately replicates the conditions of the stroma of a corneal flap resting upon the laser-modified bottom layer of corneal stroma, the obvious next tissue orientation to test engaged not just one but TWO stromal surfaces (orientation 3, stroma:stroma).

Results collected from rabbit corneas in orientation 3 (stroma:stroma) supported the hypothesis that when two stromal interfaces were allowed to interact with each other in the presence of FIB, adhesive strength doubled compared to orientation 2, in which only 1 stromal interface was exposed to the FIB glue involved in adhesion (stroma:Epi-BM). This indicates that the mechanism by which adhesion occurs is enhanced greatly when stromal ECM molecules (not laser-modified) are available on both tissue strips, when compared to orientations in which either or both strip surfaces were comprised of basement membrane ECM molecules.

Moreover, although the presence of FIB alone allowed enhanced stroma:stroma adhesion, even greater adhesion was

seen when RF and/or UVA also was present (Fig. 7c, orientation 3, protocols 6 [FIB+UVA], 8 [FIB+RF+UVA]), compared to protocol 2 (FIB alone), or protocol 5 (FIB+RF). These protocols (6 [FIB+UVA] and 8 [FIB+RF+UVA]) demonstrated more than 3× more adhesion strength in stroma:stroma orientation 3 compared to that produced when only one stromal surface was exposed to the FIB glue between them in orientation 2 (stroma:Epi-BM). In both of these cases, there is evidence of covalent and non-covalent mechanisms contributing to the substantial adhesive strength observed. Orientation 3, protocol 6 (FIB+UVA) contained FIB, which alone would produce non-covalent adhesion, based on protocol 2 (FIB) results. In addition, we hypothesized that the simplest explanation for the consistently strong adhesion of protocol 6 (FIB+UVA) was the presence of *endogenous* RF[26] (or other free radical-generating molecule, such as aromatic residues within the FIB polypeptide chain[27]) in rabbit stromas, present in a sufficient concentration to catalyze formation of UVA-catalyzed cross-linking, even in the absence of additional, exogenous RF in the FIB glue. Similarly, in protocol 8 (FIB+RF+UVA), non-covalent adhesion between stromal ECM and FIB can explain part of the overall adhesion force. Additionally, the most logical explanation for the dramatic increase in adhesion observed in orientation 3, protocol 8 (compared to protocols 2 [FIB] and 5 [FIB+RF]) is that, in addition, the formation of covalent cross-links occurs via a mechanism similar to that used to produce the strengthening effect on corneal stromal tissue itself in keratoconus RF+UVA treatment studies.[17] In our study, results from orientation 3, protocol 8 indicate that exogenous (and/or endogenous[26]) RF is activated by UVA light, releases reactive oxygen species, and thus catalyzes the formation of covalent cross-links between FIB in the glue and molecules in the corneal stroma. Finally, the great adhesion detected in orientation 3 (stroma:stroma), protocol 9, is consistent with the hypothesis of covalent cross-linking being activated, especially along the stroma-to-FIB glue interface closest to the UVA light source, because adhesion doubled when both sides of the corneal set were irradiated with UVA, thus allowing both stroma-to-FIB glue interfaces to contribute to the adhesion.

Shark cornea adhesion was tested only in the stroma:stroma orientation 3 (Fig. 8). Impressively, the results revealed adhesion strengths in the presence of FIB that were 2–2.5-fold greater than the corresponding values in rabbit stroma:stroma orientation 3 adhesion. As in the case of rabbits, shark corneas produced significantly more adhesion in those controls that contained FIB (protocols 2, 5, 6, 8, 9). This adhesive effect was non-covalent, because the adhesion in protocols 2 (FIB) and 5 (FIB+RF) occurred in the absence of UVA. Adhesion protocols 6–9 involved UVA in the presence of exogenously added RF (protocols 7–9), or hypothetically present endogenous RF or RF-like catalyzer (protocol 6).[26,27] However, those protocols generated no significantly greater adhesion than FIB alone (protocol 2) or FIB+RF (protocol 5), indicating that UVA-catalyzed adhesion did not occur between the stroma:stroma pairs. The results also suggested an absence of any *endogenous* RF-like molecules in the stroma in these shark corneas (unlike rabbit corneas), because dramatically increased adhesion was not observed in FIB+UVA (protocol 6). Unlike rabbit corneas, shark cornea adhesion was not increased markedly when cross-linking agents RF and UVA were present in the FIB-glue (protocols 8, 9). In addition, as predicted, the strength of adhesion did not double when both sides of the corneal tissue pair were irradiated for 15 minutes each with UVA (Fig. 6, protocol 9), in contrast to rabbits, therefore again suggesting no covalent interactions formed between the FIB-glue and stromal molecules in shark corneas.

Our study is intended to serve as a proof-of-concept demonstration for the ability of FIB+RF+UVA to create adhesion between two corneal stroma surfaces (neither laser-modified), and thus, adhesion between two control tissues. This work is meant to represent a first step, the required controls, in developing a treatment for post-LASIK corneas. Conditions, such as FIB concentration, RF concentration, and UVA exposure time, have yet to be optimized for use in human tissue. In addition, these same experiments using FIB+RF+UVA glue will now need to be repeated, using laser-ablated tissue, in cognizance of the altered glycosaminoglycans on such surfaces.[11] It should be noted that an RF+UVA protocol was devised recently that increased LASIK flap adhesion, but it did not involve the use of FIB[28]; neither that treatment, nor the one described here with FIB significantly alters corneal transparency.

The data from our current study revealed that FIB-mediated adhesion between a pair of stromal strips derives from formation of non-covalent and covalent bonds between the FIB-glue and ECM molecules exposed on the corneal surfaces available, with the proportion of the total strength of adhesion arising from either of those types of bonds dependent on the species of animal.

Acknowledgments

Keith Meek and Andrew Quantock of Cardiff University, Cardiff, Wales, United Kingdom, suggested, during the 2011 ARVO meeting, to remove Descemet's membrane to determine the effect of thereby exposing stromal tissue to the fibrinogen glue. Additionally, the reviewers of this study made helpful comments that allowed for the most accurate description of this study.

References

1. Jackson DW, Wang L, Koch DD. Accuracy and precision of the amadeus microkeratome in producing LASIK flaps. *Cornea*. 2003;6:504–507.
2. Jacobs BJ, Deutsch TA, Rubenstein JB. Reproducibility of corneal flap thickness in LASIK. *Ophthalmic Surg Lasers*. 1999;30:350–353.
3. Reinstein DZ, Archer TJ, Gobbe M, Johnson N. Accuracy and reproducibility of artemis central flap thickness and visual outcomes of LASIK with the Carl Zeiss Meditec VisuMax femtosecond laser and MEL 80 excimer laser platforms. *J Refract Surg*. 2010;26:107–119.
4. Talamo JH, Meltzer J, Gardner J. Reproducibility of flap thickness with IntraLase FS and Moria LSK-1 and M2 microkeratomes. *J Refract Surg*. 2006;22:556–561.
5. Cheng AC, Rao SK, Leung GY, Young AL, Lam DS. Late traumatic flap dislocations after LASIK. *J Refract Surg*. 2006; 22:500–504.
6. Kim HJ, Silverman CM. Traumatic dislocation of LASIK flaps 4 and 9 years after surgery. *J Refract Surg*. 2010;26:447–452.
7. Ramírez M, Quiroz-Mercado H, Hernandez-Quintela E, Naranjo-Tackman R. Traumatic flap dislocation 4 years after LASIK due to air bag injury. *J Refract Surg*. 2007;23:729–730.
8. Aldave AJ, Hollander DA, Abbott RL. Late-onset traumatic flap dislocation and diffuse lamellar inflammation after laser in situ keratomileusis. *Cornea*. 2002;21:604–607.
9. Caster AI, Friess DW, Schwendeman FJ. Incidence of epithelial ingrowth in primary and retreatment laser in situ keratomileusis. *J Cataract Refract Surg*. 2010;36:97–101.
10. Mohamed TA, Hoffman RS, Fine IH, Packer M. Post-laser assisted in situ keratomileusis epithelial ingrowth and its relation to pretreatment refractive error. *Cornea*. 2011;30: 550–552.

11. Zhang Y, Schmack I, Dawson DG, et al. Keratan sulfate and chondroitin/dermatan sulfate in maximally recovered hypocellular stromal interface scars of postmortem human LASIK corneas. *Invest Ophthalmol Vis Sci*. 2006;47:2390–2396.
12. Khadem J, Truong T, Ernest JT. Photodynamic biologic tissue glue. *Cornea*. 1994;13:406–410.
13. Goldman JN, Benedek GB. The relationship between morphology and transparency in the nonswelling corneal stroma of the shark. *Invest Ophthalmol*. 1967;6:574–600.
14. Conrad AH, Zhang Y, Walker AR, et al. Thyroxine affects expression of KSPG-related genes, the carbonic anhydrase II gene, and KS sulfation in the embryonic chicken cornea. *Invest Ophthalmol Vis Sci*. 2006;47:120–132.
15. Spoerl E, Mrochen M, Sliney D, Trokel S, Seiler T. Safety of UVA-riboflavin cross-linking of the cornea. *Cornea*. 2007;26:385–389.
16. Brummer G, Littlechild S, McCall S, Zhang Y, Conrad GW. The role of nonenzymatic glycation and carbonyls in collagen cross-linking for the treatment of keratoconus. *Invest Ophthalmol Vis Sci*. 2011;52:6363–6369.
17. McCall AS, Kraft S, Edelhauser HF, et al. Mechanisms of corneal tissue cross-linking in response to treatment with topical riboflavin and long wavelength ultraviolet radiation (UVA). *Invest Ophthalmol Vis Sci*. 2010;51:129–138.
18. Griffith M, Jackson WB, Lafontaine MD, Mintsioulis G, Agapitos P, Hodge W. Evaluation of current techniques of corneal epithelial removal in hyperopic photorefractive keratectomy. *J Cataract Refract Surg*. 1998;24:1070–1078.
19. Fujikawa LS, Foster CS, Gipson IK, Colvin RB. Basement membrane components in healing rabbit corneal epithelial wounds: immunofluorescence and ultrastructural studies. *J Cell Biol*. 1984;98:128–138.
20. Grant DS, Leblond CP. Immunogold quantitation of laminin, type IV collagen, and heparan sulfate proteoglycan in a variety of basement membranes. *J Histochem Cytochem*. 1988;36:271–283.
21. Timpl R, Rohde H, Robey PG, Rennard SI, Foidart JM, Martin GR. Laminin–a glycoprotein from basement membranes. *J Biol Chem*. 1979;254:9933–9937.
22. Ratkay-Traub I, Juhasz T, Horvath C, et al. Ultra-short pulse (femtosecond) laser surgery: initial use in LASIK flap creation. *Ophthalmol Clin North Am*. 2001;14:347–355.
23. von Jagow B, Kohnen T. Corneal architecture of femtosecond laser and microkeratome flaps imaged by anterior segment optical coherence tomography. *J Cataract Refract Surg*. 2009;35:35–41.
24. Lee RE, Davison PF. Collagen composition and turnover in ocular tissues of the rabbit. *Exp Eye Res*. 1981;32:737–745.
25. Michelacci YM. Collagens and proteoglycans of the corneal extracellular matrix. *Braz J Med Biol Res*. 2003;36:1037–1046.
26. Bessey OA, Lowry OH. Factors influencing the riboflavin content of the cornea. *J Biol Chem*. 1944;155:635–643.
27. Cornwell KG, Pins GD. Discrete crosslinked fibrin microthread scaffolds for tissue regeneration. *J Biomed Mater Res A*. 2007;82:104–112.
28. Mi S, Dooley EP, Albon J, Boulton ME, Meek KM, Kamma-Lorger CS. Adhesion of laser in situ keratomileusis-like flaps in the cornea: Effects of crosslinking, stromal fibroblasts, and cytokine treatment. *J Cataract Refract Surg*. 2011;37:166–172.